Pramana – J. Phys. (2019) 93:18
https://doi.org/10.1007/s12043-019-1775-6

Ab initio study of the fundamental properties of $Zn_{1-x}TM_xSe$ (TM=Mn, Co and Fe)

F SOLTANI[1], H BAAZIZ[2,3,*], Z CHARIFI[2,3], F EL HAJ HASSAN[4] and B HAMAD[5,6]

[1]Department of Physics, Faculty of Science, University of Batna, 050 00 Batna, Algeria
[2]Department of Physics, Faculty of Science, University of M'sila, 28000 M'sila, Algeria
[3]Laboratory of Physics and Chemistry of Materials, University of M'sila, M'sila, Algeria
[4]Université Libanaise, Faculté des Sciences (I), Laboratoire de Physique et d'Electronique (LPE), Elhadath, Beirut, Lebanon
[5]Department of Physics, The University of Jordan, Amman 11942, Jordan
[6]Department of Physics, University of Arkansas, Fayetteville, AR 72701, USA
*Corresponding author. E-mail: baaziz_hakim@yahoo.fr

MS received 25 June 2018; revised 16 December 2018; accepted 4 January 2019; published online 21 May 2019

Abstract. The structural, electronic, magnetic, thermal and elastic properties of $Zn_{1-x}TM_xSe$ (TM = Mn, Co and Fe) ternary alloys are investigated at x = 0, 0.25, 0.50, 0.75 and 1.00 in the zincblende (B3) phase. The calculations are performed using all-electron full-potential linearised augmented plane-wave (FP-LAPW) method within the framework of the density functional theory (DFT) and the generalised gradient approximation (GGA). The electronic and magnetic properties were performed using the modified Becke–Johnson potential combined with the GGA correlation (mBJ-GGA). The electronic structures are found to exhibit a semiconducting behaviour for $Zn_{1-x}Mn_xSe$ and $Zn_{1-x}Co_xSe$ and a half-metallic behaviour for $Zn_{1-x}Fe_xSe$ alloys at all concentrations, while CoSe with $x = 1.00$ is found to exhibit a metallic behaviour. The calculated magnetic moment per substituted transition metal (TM) Mn, Co and Fe atoms for half-metallic compounds are found to be 2.5, 1.5 and 2 μ_B, respectively. The p–d hybridisation between the TM d- and Se p-states reduces the local magnetic moment of Mn, Co and Fe and induces small local magnetic moments on Zn and Se sites. In addition, we discuss the mechanical behaviour of binary and ternary compounds and all compounds studied here are mechanically stable.

Keywords. Density functional theory; magnetic semiconductor; electronic structure; magnetic properties; spintronics.

PACS Nos 71.15.Mb; 71.15.−m; 65.40.Ba; 71.10.Hf; 65.40.gd

1. Introduction

The use of the spin of electron in information technology, in addition to the electric charge, creates a new field of physics called 'spintronics' [1,2]. This field of research promises to evolve towards applications in optoelectronics and quantum information [3]. The expected benefits of increasing the speed of data processing and reducing the energy consumption of future spintronic devices are attracting the attention of major research laboratories as well as industries. The diluted magnetic semiconductors (DMSs) are the most promising materials to realise these types of devices. The doping of a semiconductor with a magnetic element is likely to confer the properties of a ferromagnetic material, while maintaining the semiconductor character. The gain of the magnetic properties makes it possible to manipulate the state of spin of the carriers and the density of the carriers by means of magnetic and electric fields [4]. The DMSs based on II–VI semiconductors such as ZnO and ZnS have been widely studied for their wide band-gap character [5,6]. Their band-gap energy falls between 1 and 3 eV, which makes them useful in optoelectronic devices in the visible region of the spectrum [7]. The DMSs II-TM-VI [8] are formed by randomly replacing a fraction of the cations in binary semiconducting alloys with magnetic ions. These materials display an exchange interaction between the localised magnetic moment and the electron bands. Many research teams have theoretically predicted

different binary semiconductors doped with transition metals (TMs) such as doping BeSe and BeTe with Cr [9], CdS with Fe [10], MgSe, MgTe and CdTe with V [11,12], and ZnO with V, Cr, Mn, Fe and Co [13]. Zinc selenide (ZnSe) is a very interesting material for both ultraviolet (UV) and infrared (IR) applications [14] and is suitable for short-wavelength optoelectronic devices [15]. This compound is reported to crystallise in zincblende (ZB)- and wurtzite (WZ)-type structures [16].

In this paper, we investigate the structural, electronic, magnetic, thermal and elastic properties of ZnSe doped by Mn, Fe and Co elements. The remaining part of the paper is organised as follows: Section 2 includes the computational details, §3 contains the results and discussion and §4 summarises the concluding remarks.

2. Computational details

The calculations are performed using the full potential linearised augmented plane-wave (FP-LAPW) method [17] to solve the Kohn–Sham equation [18] as implemented in Wien2k code [19] within the density functional theory (DFT) [20]. The exchange-correlation potential for structural properties is described within the generalised gradient approximation (GGA) proposed by Perdew *et al* [21]. The calculated total energy–volume (E–V) data are fitted to the Birch Murnaghan equation of state [22]. For the electronic properties, we applied the Engel–Vosko generalised gradient approximation (EV-GGA) [23] and the modified Becke–Johnson generalised gradient approximation (mBJ-GGA) [24] schemes. ThemBJ-GGA approximation is a new potential that depends solely on semilocal quantities. The muffin-tin sphere radii are selected to be 2.1 a.u. for Zn, Mn, Fe and Co atoms and 1.9 a.u. for Se atom. Ak-mesh of 11 × 11 × 11 is used to guarantee convergence in the Brillouin zone integration. The plane-wave cut-off of $K_{\max} = 8.0/R_{\mathrm{MT}}$ is chosen for expansion of wave functions in the interstitial region of the alloys. The charge density is Fourier-expanded up to $G_{\max} = 12$ Ry. ZnSe has a ZB structure with a space group of $F\bar{4}3m$ and its experimental lattice constant is 5.668 Å [25]. The DMSs $Zn_{1-x}TM_xSe$ (TM = Mn, Co and Fe) compounds are formed by randomly replacing Zn atoms with magnetic ions at concentrations of $x = 0.25$, 0.5 and 0.75. For this purpose, we used the conventional unit cell with eight atoms with a space group $P43m$. Thus, $x = 0.25$ concentration is obtained by replacing one atom of Zn by Mn, Co or Fe at compatible sites. In the same way, we attain $x = 0.5$ and 0.75 by substituting two and three atoms of Zn, respectively, at compatible sites. The crystallographic structures of the $Zn_{1-x}TM_xSe$ alloys are presented in figure 1. The thermodynamic properties are studied using the quasiharmonic Debye model and the elastic properties are calculated using the Voigt, Reuss and Hill approximations.

3. Results and discussion

3.1 *Structural properties*

The crystal structures of bulk ZnSe, MnSe, CoSe and FeSe are ZB, rock salt, NiAs hexagonal type and PbO tetragonal type, respectively. Although only ZnSe has a ZB structure, the other three alloys are believed to have metastable structures that make them interesting to be grown on semiconducting substrates using molecular beam epitaxy (MBE). The rocksalt structure of MnSe is compatible with the ZB structure as reported in [26,27]. Therefore, it could be fabricated using MBE in the ZB structure to form ZnSe/MnSe superlattices [28]. Similarly, CoSe and FeSe have NiAs structure that could also be prepared in ZB structures using MBE to be deposited on substrates of ZB structures such as (0 0 1) GaAs. Thus, the structural properties of ZnSe, MnSe, CoSe and FeSe binary compounds were calculated in their ZB structure. The ternary alloys were modelled with some selected compositions by randomly

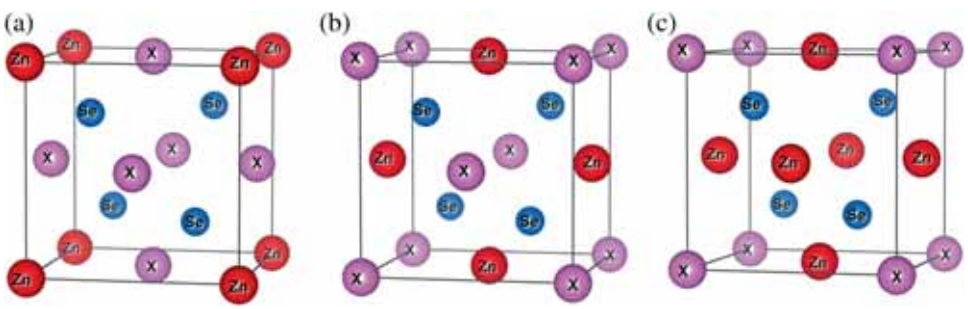

Figure 1. Representation of the crystallographic structure of $Zn_{1-x}TM_xSe$: (**a**) $x = 0.75$, (**b**) $x = 0.5$ and (**c**) $x = 0.25$.

Table 1. Calculated equilibrium lattice parameter a_0 (Å), bulk modulus B (GPa) and cohesive energy (E_{coh}) for $Zn_{1-x}Mn_xSe$, $Zn_{1-x}Co_xSe$ and $Zn_{1-x}Fe_xSe$ alloys using GGA approximation.

Alloys	x	Lattice constants a (Å)				Bulk modulus B(GPa)			E_{coh}	
		Our work	Vegard's law	Exp.	Other works	Our work	Exp.	Other works	Our works	Other works
$Zn_{1-x}Mn_xSe$	0	5.754		5.668[a]	5.630[b], 5.624[c], 5.75[d], 5.667[e], 5.79[f]	57.310	69.3[b], 64.7[d]	63.34[b], 71.82[c], 59.0[e], 59.0175[f], 57.30[d]	2.432	−2.287[e], 2.19[expj]
	0.25	5.781	5.70[g]			54.789			5.378	
	0.50	5.831	5.74[g]			53.274			5.871	
	0.75	5.889	5.78[g]			51.451			6.352	
	1	5.949			5.820[cif+h]	45.955			3.411	
$Zn_{1-x}Co_xSe$	0	5.754		5.668[a]		57.310	69.3[b]	63.34[b]	2.432	2.19[expj]
	0.25	5.701	5.576[g]			58.453			5.624	
	0.50	5.660	5.484[g]			54.855			6.385	
	0.75	5.513	5.392[g]			55.360			7.215	
	1	5.287				99.434			4.110	
$Zn_{1-x}Fe_xSe$	0	5.754		5.668[a]	5.630[b], 5.624[c]	57.310	69.3[b]	63.34[b]	2.432	2.19[expj]
	0.25	5.733	5.705[g]			57.615			5.838	
	0.50	5.728	5.743[g]			56.739			6.776	
	0.75	5.686	5.780[g]			52.361			7.732	
	1	5.627		5.818[h]	5.818[h]	47.310			4.365	

[a]Ref. [25], [b]ref. [30], [c]ref. [31], [d]ref. [32], [e]ref. [33], [f]ref. [34], [g]ref. [29] calculated lattice constant of alloys with Vegard's law, [h]ref. [35], [j]ref. [36].

Table 2. Direct and indirect band-gap energies, majority-spin $N^{\uparrow}(E_F)$, minority-spin $N^{\downarrow}(E_F)$ states, the spin polarisation P and half-metallic gaps G^{HM} for $Zn_{1-x}Mn_xSe$, $Zn_{1-x}Co_xSe$ and $Zn_{1-x}Fe_xSe$ using mBJ-GGA and EV-GGA approximations.

Compounds	x	E_g (eV) Γ−Γ			E_g (eV) M−M	E_g (eV) Γ−M			G^{HM}	$N^{\uparrow}(E_F)$(States/eV)	$N^{\downarrow}(E_F)$(States/eV)	P
		This work				Others			This work			
		GGA	mBJ-GGA	EV-GGA	GGA	mBJ-GGA	EV-GGA		mBJ-GGA			
$Zn_{1-x}Mn_xSe$	0	1.092	2.576	1.850				1.31[a], 2.82[expb] 1.017[c], 1.029[c]		0.05	0.05	–
	0.25	1.986	3.119	2.524					1.039	1.18	0.00	1
	0.5	2.187	3.138	2.5530					1.680	0.71	0.00	1
	0.75	2.371	3.346	2.744					2.221	0.84	0.00	1
	1	3.555	4.4272	3.83					2.703	0.02	0.00	1
$Zn_{1-x}Co_xSe$	0	1.092	2.576	1.850				1.31[a], 2.82[expb] 1.017[c], 1.029[c]		0.05	0.05	
	0.25	****	2.397	1.032	0.540				0.496	1.08	0.00	1
	0.5	0.222	****	****		2.106	0.714		0.710	0.74	0.00	1
	0.75		****			2.196			1.464	1.06	0.00	1
	1								4.86	9.74	0.33	
$Zn_{1-x}Fe_xSe$	0	1.092	2.576	1.850				1.31[a], 2.82[expb] 1.017[c], 1.029[c]		0.05	0.05	
	0.25	0.893	2.381	1.672					0.708	0.00	115.80	1
	0.5	0.773	2.195	1.517					0.296	0.37	0.00	1
	0.75	0.837	2.186	1.672					0.503	0.00	20.59	1
	1	0.870	2.358	1.890					0.148	0.00	26.18	1

[a]Ref. [32], [b]ref. [38], [c]ref. [35].

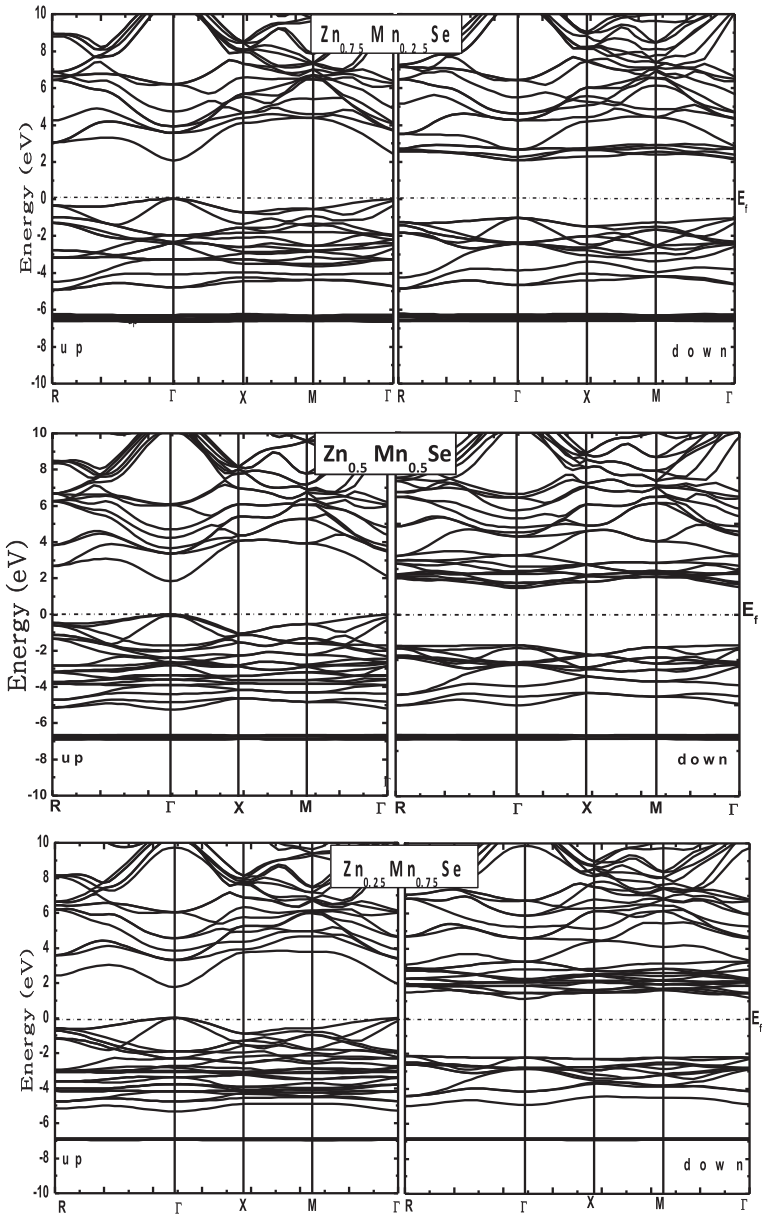

Figure 2. Spin-polarised electronic band structure for $Zn_{1-x}Mn_xSe$ alloys when $x = 0.25$, 0.50 and 0.75 using mBJ-GGA approximation.

replacing a fraction of cations ($x = 0.25$, 0.5 and 0.75) in the binary compounds. Following Vegard's law [29], the lattice constant of the ternary alloy can be obtained from those of the binary alloys as follows:

$$a_{(Zn_{1-x}TM_xSe)} = (1-x)a_{ZnSe} + xa_{TMSe}, \quad (1)$$

where a_{ZnSe} and a_{TMSe} are the equilibrium lattice constants of ZnSe and TMSe binary compounds, respectively, whereas $a_{(Zn1-xTMxSe)}$ is the lattice constant of the ternary alloy.

We calculated the variation of total energy with the cell volume of ZnSe and $Zn_{1-x}TM_xSe$ (TM = Mn, Co and Fe) compounds using GGA approximation. We summarised our results and the available experimental and other theoretical values, as shown in table 1. The obtained results for pure ZnSe are compared with the experimental data and other published theoretical calculations. However, it was not possible to make any comparison for $Zn_{1-x}Mn_xSe$, $Zn_{1-x}Co_xSe$ and $Zn_{1-x}Fe_xSe$ as there was no experimental data. It is interesting to note that for $Zn_{1-x}Mn_xSe$, the lattice parameter increases when x varies from 0.25 to 0.75. In addition, the bulk modulus decreases with x varying from 0.25 to 0.75. For $Zn_{1-x}Co_xSe$ and $Zn_{1-x}Fe_xSe$, the lattice parameter decreases when x varies from 0.25 to 0.75, while the bulk modulus increases as well as

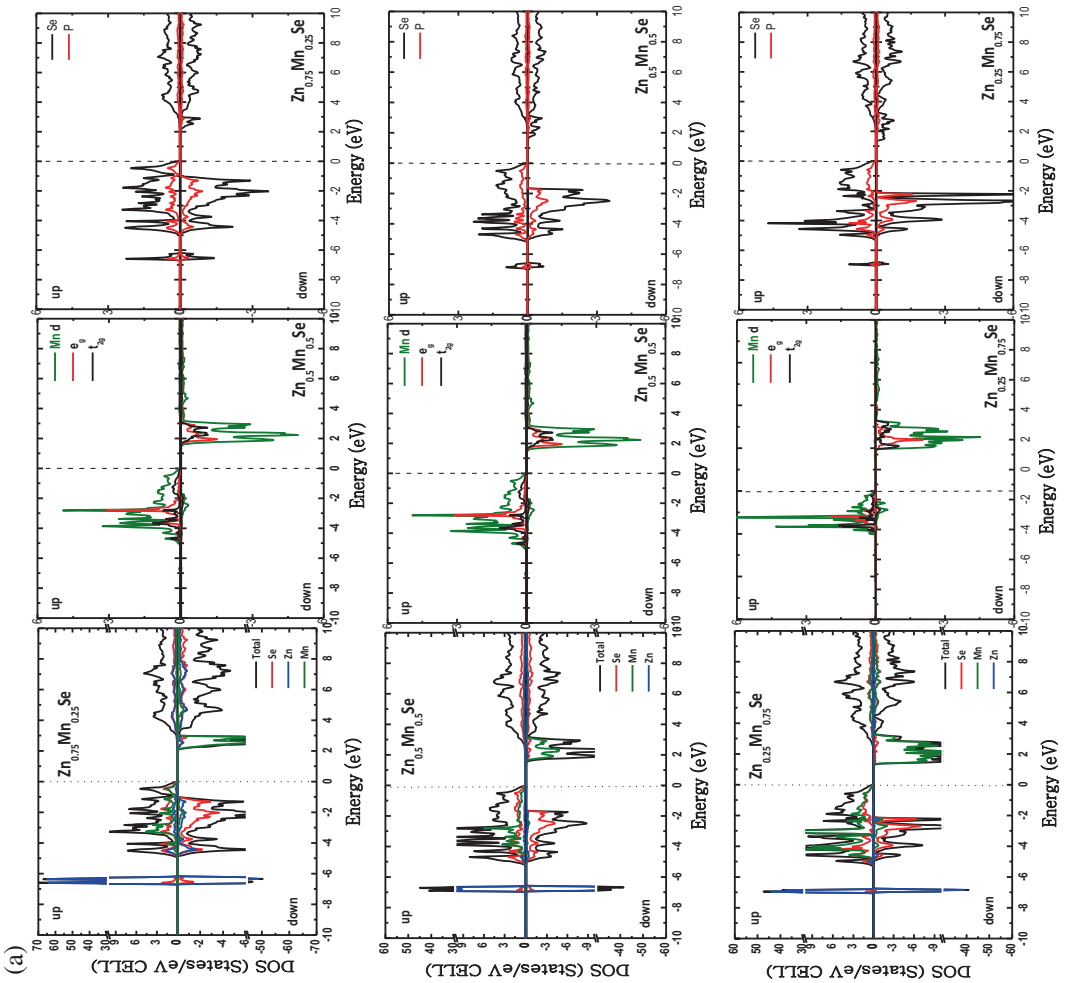
(a)
DOS (States/eV CELL)
Energy (eV)
Zn0.75Mn0.25Se
Zn0.5Mn0.5Se
Zn0.25Mn0.75Se
Total
Se
Zn
Mn
Mn d
eg
t2g
P
up
down

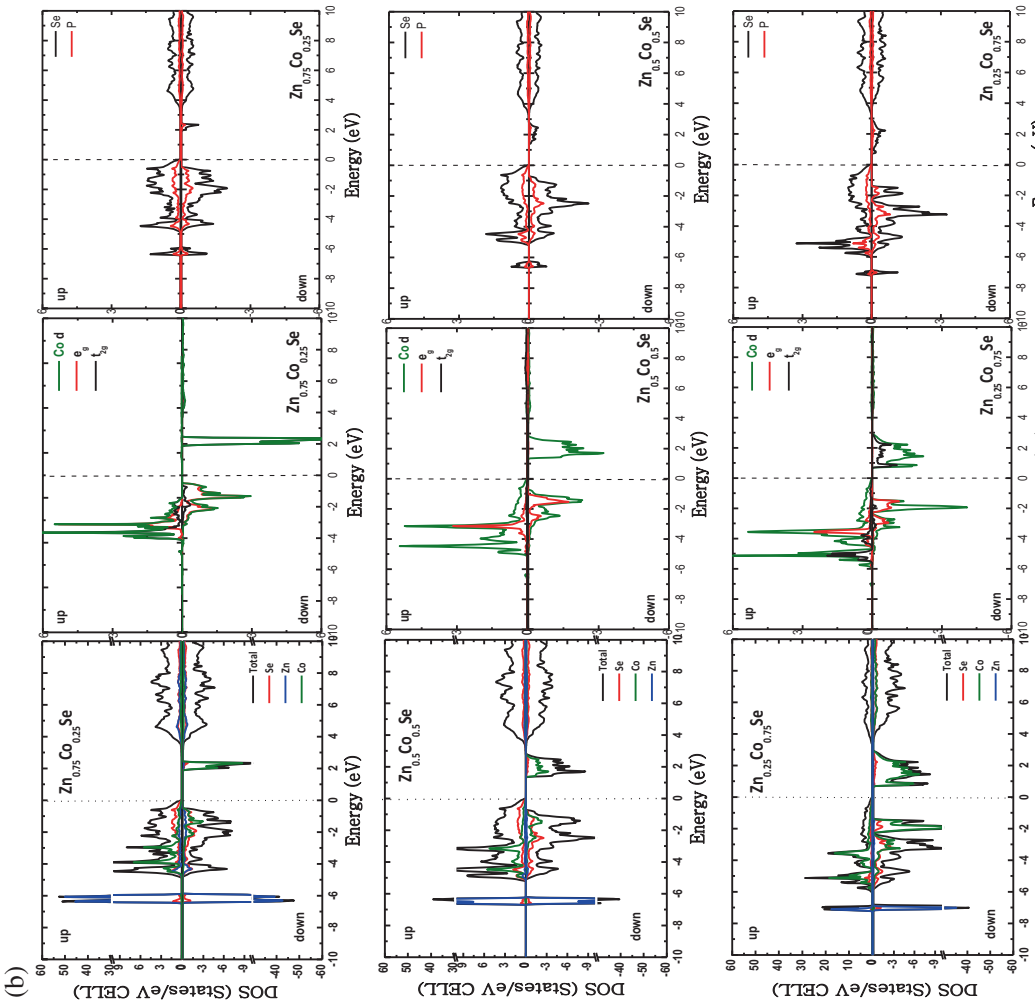

Figure 3. Density of states for $Zn_{1-x}Mn_xSe$, $Zn_{1-x}Co_xSe$ and $Zn_{1-x}Fe_xSe$ alloys when $x =$ (**a**) 0.25, (**b**) 0.50 and (**c**) 0.75 using mBJ-GGA approximation.

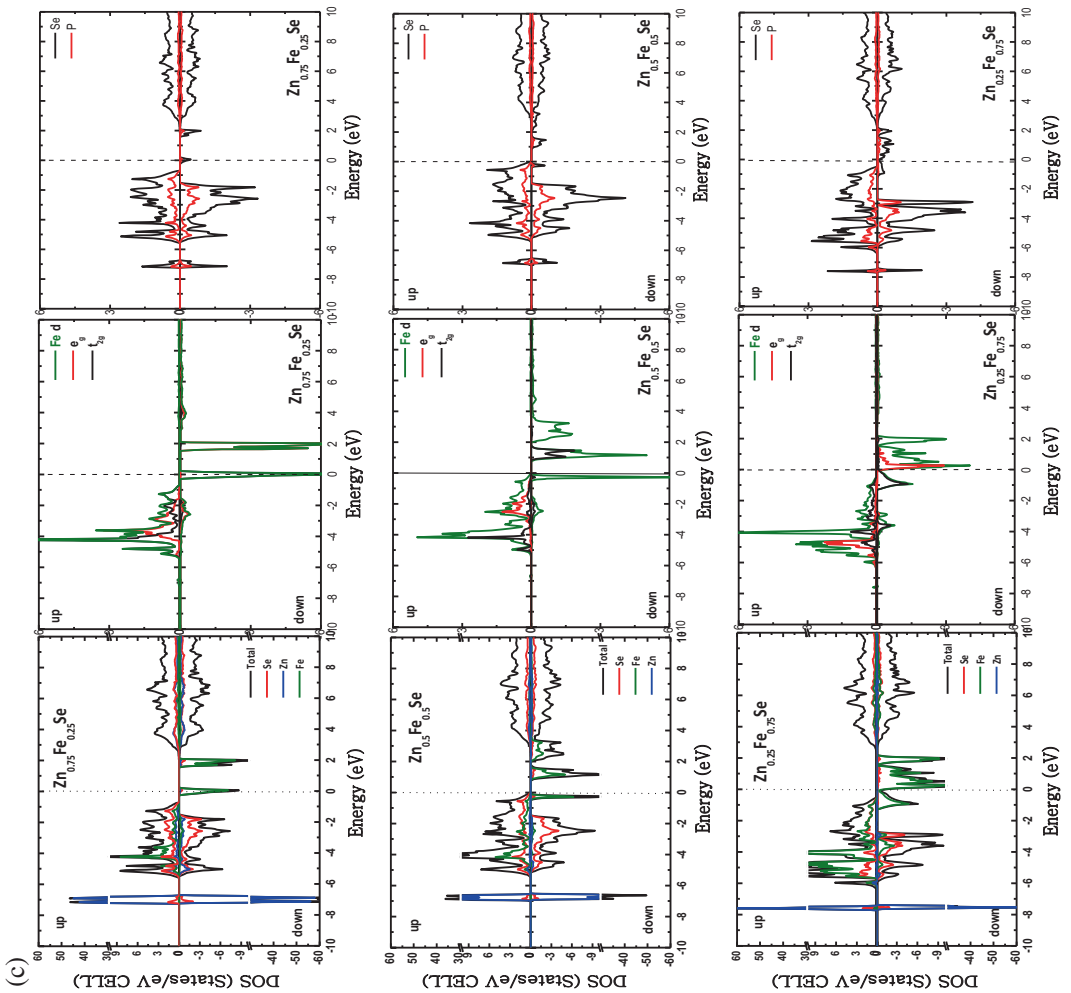

Figure 3. *Continued.*

decreases when x varies from 0.25 to 0.75. Certainly, the effect of Co, Fe and Mn doping decreases or increases the lattice constant, because the lattice parameters are controlled by the relative size of the atoms or species exchanged. For this increase or decrease of lattice parameters, our calculations are in agreement with Vegard's law [37].

In addition, the cohesive energy of these compounds is calculated using the following equation:

$$E_{\text{coh}} = \sum_i E_i - E_{\text{tot}}, \tag{2}$$

where E_{tot} is the total energy of $Zn_{1-x}TM_xSe$ ternary alloys at their equilibrium lattice constants and $\sum_i E_i$ is the sum of the total energies of the isolated atoms in each compound [30].

The structural parameters and cohesive energies of the alloys are listed in table 1. Our results for ZnSe are found to be in a good agreement with the experimental findings [25] and previous calculations [31–35]. The lattice constant is found to be larger than the experimental value by 1.5% [24], whereas the bulk modulus is less than the reported experimental values by 17% [30] and 11% [33]. Moreover, our results are found to be in agreement with previous theoretical predictions [31–35].

3.2 *Electronic properties*

The results of the calculated band structure are presented in table 2. The spin-polarised band structure calculations using GGA, EV-GGA and mBJ-GGA functionals predict direct band gaps, E_g, at the Γ high symmetry point. It is well known that GGA usually underestimates the energy gap [39,40], whereas the values given by mBJ-GGA are in good agreement with the experimental data. As a prototype, figure 2 shows the band structure of $Zn_{1-x}Mn_xSe$ (spin-up and spin-down). Accordingly, one can perceive a nearly metallic behaviour due to some electrons in the majority-spin (spin-up), whereas the minority-spin (spin-down) channel exhibits semiconducting behaviour at different concentrations. The half-metallic gap (G_{HM}) is defined as the minimum between the lowest energy of the majority (minority) spin conduction bands with respect to the Fermi level and the absolute values of the highest energy of majority (minority) spin valence [41]. The calculated G_{HM} values are shown in table 2. The spin polarisation of systems at the Fermi level is calculated using the following equation:

$$p = \frac{N^{\uparrow}(E_{\text{F}}) - N^{\downarrow}(E_{\text{F}})}{N^{\uparrow}(E_{\text{F}}) + N^{\downarrow}(E_{\text{F}})}, \tag{3}$$

where $N^{\uparrow}(E_{\text{F}})$ and $N^{\downarrow}(E_{\text{F}})$ are defined as the number of states at the majority-spin and minority-spin channels, respectively.

The projected density of states of $Zn_{1-x}Mn_xSe$ compounds is shown in figure 3a. The valence bands in the ranges (−7.04, −5.96 eV), (−7.28, −6.15 eV) and (−7.078, −6.61 eV) at $x = 0.25$, 0.5 and 0.75, respectively, originate from Zn-d states and the small contribution from the Se-s states. However, the intermediate part of the valence band among −5.042, −5.248 and −5.29 eV and the Fermi level for $Zn_{0.75}Mn_{0.25}Se$, $Zn_{0.5}Mn_{0.5}Se$ and $Zn_{0.25}Mn_{0.75}Se$, respectively, originate from Se-p, Zn-s and Mn-3d states, respectively. One can also see from figure 3a that the higher part of the valence band of the majority spin is mainly generated from Mn-3d states with a small contribution of Se-p and Zn-s with few electronic states at the Fermi level that leads to an early metallic behaviour. However, in the minority spin case, the lower part of the conduction band is dominated by Mn-3d states within the range (1.86, 3.29 eV), (1.32, 3.4 eV) and (1.21, 3.66 eV) at $x = 0.25$, 0.50 and 0.75, respectively, with a small contribution of Se-p states. However, no states are found at the Fermi level, confirming its semiconducting behaviour. Therefore, these compounds are considered to exhibit semiconducting behaviour. Similarly, $Zn_{1-x}Co_xSe$ alloys show semiconducting behaviour in the spin-down and spin-up channels (see figure 3b). The second region close to the Fermi level is dominated by the Co-3d orbital with a small contribution of Se-p and Zn-s states. Furthermore, the $Zn_{1-x}Fe_xSe$ alloys are semiconducting at $x = 0.5$ and half metallic at $x = 0.25$ and 0.75 (see figure 3c). The conduction band is dominated mainly by the contribution of the Fe-3d orbital and a small contribution of s, p and d orbitals of Se and Zn atoms. This separation in energy is due to the strong p–d exchange interaction between the 3d states of Fe atoms and the anion at the p orbitals. This hybridisation is responsible for creating a half-metal (HM) gap in these compounds. We also predicted CoSe as a metal with a spin polarisation of 33%. It is clearly seen that the results of the spin polarisation confirm the type of alloys as HM or semiconductors. The energy bands are the result of the contributions of the d orbital of Zn atom with a small contribution of the s and p orbitals of Se atom.

3.3 *Magnetic properties*

The calculated total and local magnetic moments for $Zn_{1-x}TM_xSe$ compounds are presented in table 3. The TMs in the ternary compounds have tetrahedral configurations that lead to e_g, t_{2g} splitting of the

Table 3. Calculated total and partial magnetic moments $m^{tot}(\mu_B)$ for $Zn_{1-x}Mn_xSe$, $Zn_{1-x}Co_xSe$ and $Zn_{1-x}Fe_xSe$ alloys using GGA and mBJ-GGA approximations.

Compounds	x	$M_s(\mu_B)$									
		This work									
		M^{tot} (μ_B)		m^{Zn} (μ_B)		m^{Mn} (μ_B)		m^{Se} (μ_B)			
		GGA	mBJ-GGA	GGA	mBJ-GGA	GGA	mBJ-GGA	GGA	mBJ-GGA	MMINT-GGA	MMINTmBJ-GGA
$Zn_{1-x}Mn_xSe$	0	0.000	0.000	−0.000	−0.000			0.000	0.000	0.000	0.000
	0.25	1.250	1.250	0.027	0.017	1.060	1.077	0.035	0.026	0.532	0.533
	0.5	2.500	2.500	0.043	0.032	1.055	1.088	0.055	0.048	1.256	1.033
	0.75	3.750	3.750	0.059	0.053	1.068	1.118	0.073	0.074	1.832	1.233
	1	5.000	5.000			4.318	4.542	0.095	0.097	0.586	0.361
		M^{tot} (μ_B)		m^{Zn} (μ_B)		m^{Co} (μ_B)		m^{Se} (μ_B)			
		GGA	mBJ-GGA	GGA	mBJ-GGA	GGA	mBJ-GGA	GGA	mBJ-GGA		
$Zn_{1-x}Co_xSe$	0	0.000	0.000	−0.000	−0.000			−0.000	0.000	0.000	0.000
	0.25	0.750	0.750	0.013	0.006	0.569	0.637	0.055	0.031	0.459	0.305
	0.5	1.500	1.500	0.020	0.013	0.591	0.639	0.096	0.060	0.846	0.619
	0.75	1.540	2.250	0.028	0.029	0.437	0.658	0.058	0.095	0.650	0.994
	1	0.203	2.668			0.137	2.304	0.003	0.092	0.008	0.011
		M^{tot} (μ_B)		m^{Zn} (μ_B)		m^{Fe} (μ_B)		m^{Se} (μ_B)			
		GGA	mBJ-GGA	GGA	mBJ-GGA	GGA	mBJ-GGA	GGA	mBJ-GGA		
$Zn_{1-x}Fe_xSe$	0	0.000	0.000	−0.000	−0.000			−0.000	0.000	0.000	0.000
	0.25	1.000	1.000	0.019	0.012	0.831	0.877	0.061	0.045	0.372	0.267
	0.5	2.000	2.000	0.043	0.030	0.840	0.868	0.112	0.070	0.741	0.715
	0.75	2.903	3.000	0.051	0.049	0.843	0.893	0.146	0.136	0.852	0.676
	1	3.659	4.000			3.268	3.574	0.136	0.222	0.255	0.202

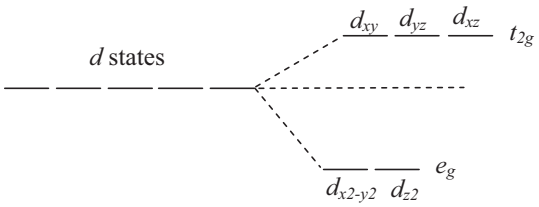

Figure 4. Schematic crystal field splitting of the d-orbital in the tetrahedral configuration.

d-orbitals (see figure 4). The electronic configurations of these metals are $Mn^{2+}(d^5–e_g^2t_{2g}^3)$, $Co^{2+}(d^7–e_g^4t_{2g}^3)$ and $Fe^{2+}(d^6–e_g^3t_{2g}^3)$. Hence, the spin-up states of Mn, Co and Fe are filled, whereas the spin-down states are unoccupied for Mn and partially occupied for Co and Fe. The hybridisation between the Se-p states and Mn, Co/Fe-d states reduces the total magnetic moments of Mn, Co and Fe and from their free space charge value and produces small local magnetic moments on the non-magnetic Zn and Se sites. The substitutional doping of Mn, Co and Fe ions at the Zn site modifies the number of majority-spin and minority-spin states in the valence band of ZnSe: the majority-spin states of Mn, Co and Fe are filled, the minority-spin states of Co/Fe are partially occupied, whereas those of Mn are empty. As a result, in the case of semiconducting majority spin, Se ion states become more occupied than the minority-spin states. Hence, induced magnetic moments in Se ions are parallel to those of Co/Fe ions for $Zn_{1-x}Co_xSe/Zn_{1-x}Fe_xSe$/compounds. In the same way, the Zn cations interact with Se ions and as a result the magnetic coupling of Zn and Se is also ferromagnetic. However, in the case of the $Zn_{1-x}Mn_xSe$ compounds, the sign of the magnetic moments on Se and Zn is generally opposite to that on Mn, Co/Fe, which means that the valence band carriers, having mainly Se-p character, interact antiferromagnetically with Mn, Co/Fe spins. The total magnetic moments are found to increase by increasing the fraction x of $Zn_{1-x}Mn_xSe/Zn_{1-x}Fe_xSe$. This increase depends on the number of valence electrons that causes an energy shift of the partial densities. The calculated total magnetic moments of the $Zn_{1-x}Mn_xSe$ compounds at $x = 0.25$, 0.5 and 0.75 are found to be 1.25, 2.5 and 3.75 μ_B, respectively. However, for $Zn_{1-x}Co_xSe$, the magnetic moments are 0.75, 1.5 and 1.54 μ_B, whereas they are found to be 1.0, 2.0 and 2.90 μ_B for the $Zn_{1-x}Fe_xSe$ compound at $x = 0.25$, 0.5 and 0.75, respectively. It is interesting to note that the total

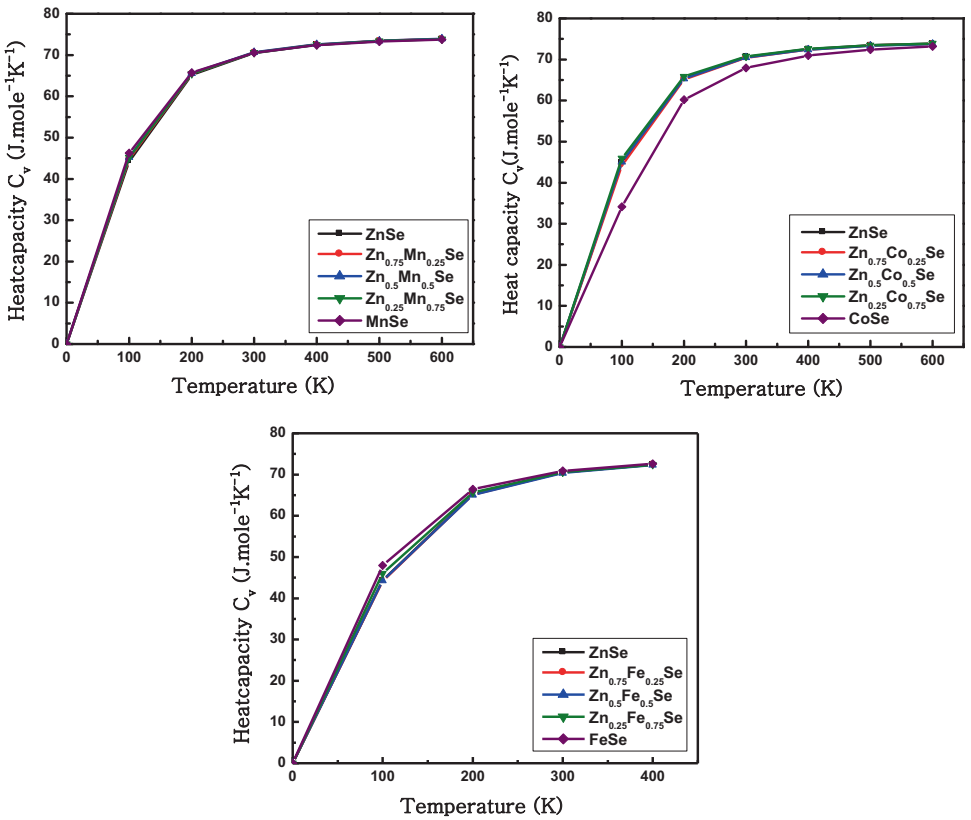

Figure 5. The heat capacity C_v as a function of concentration x for $Zn_{1-x}Mn_xSe$, $Zn_{1-x}Co_xSe$ and $Zn_{1-x}Fe_xSe$ alloys when $x = 0.25$, 0.50 and 0.75 at various temperatures.

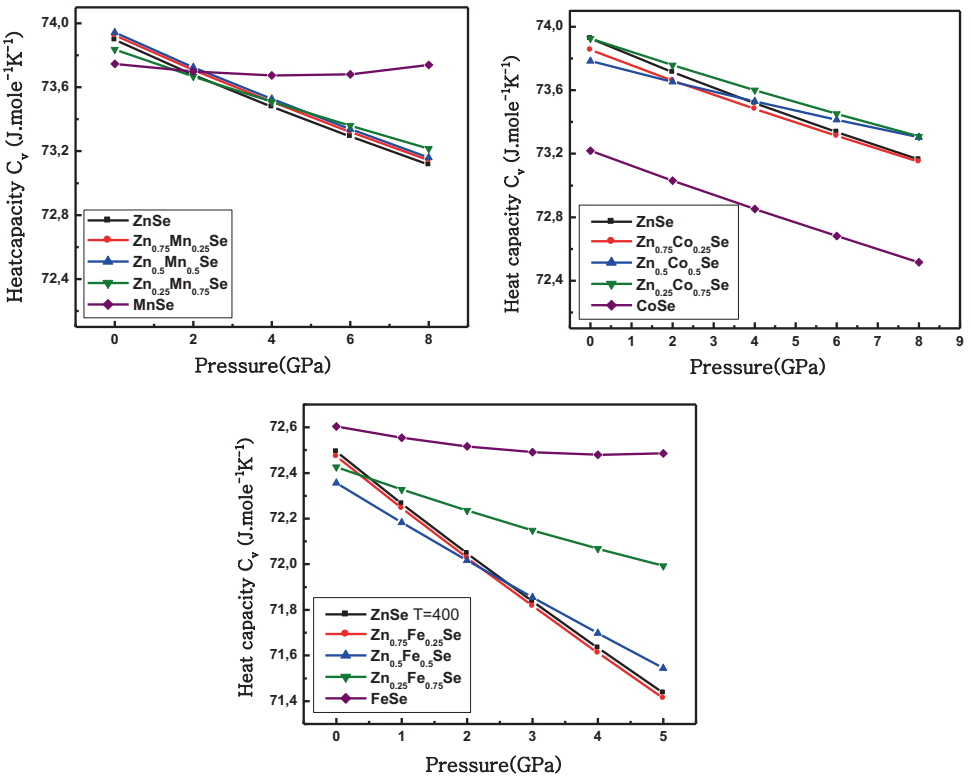

Figure 6. The heat capacity C_v as a function of concentration x for $Zn_{1-x}Mn_xSe$, $Zn_{1-x}Co_xSe$ and $Zn_{1-x}Fe_xSe$ alloys when $x = 0.25$, 0.50 and 0.75 at various pressures.

magnetic moments increase with respect to x in all compounds.

3.4 *Thermodynamic properties*

We used the quasiharmonic model [42] as implemented in the Gibbs2 program [42,43]. Using this model, one can calculate the thermal properties at different temperatures and pressures. The temperature ranges from 0 to 600 K and the pressure ranges from 0 to 8 GPa. The determination of the heat capacity is useful for many applications. The heat capacity was found to increase rapidly at low temperatures and then converge to Delong–Petit limit at high temperature as shown in figure 5. In addition, the heat capacity at constant volume, C_v, decreases almost linearly as a function of pressure (see figure 6).

3.5 *Elastic properties*

The elastic properties reflect the response of the interatomic forces by taking into account the stress and the structural stability based of Hooke's law. In the symmetry of cubic materials, only three independent elastic constants are needed: C_{11}, C_{12} and C_{44}. The mechanical stability of the cubic crystal must satisfy the Born stability criteria [44] as follows:

$$(C_{11} - C_{12}) > 0, \quad C_{44} > 0, \quad (C_{11} + 2C_{12}) > 0. \quad (4)$$

The calculated elastic values are tabulated in tables 4 and 5. According to the Born's stability criteria, it can be noted that the binary and ternary alloys are mechanically stable. The compounds studied are highly resistant when compared with unidirectional materials because C_{11} is larger than C_{12} and C_{44}.

In the Voigt–Reuses–Hill approximation [48–50], A is the anisotropic factor, C_s represents the resistance to the shear strain, B is the bulk modulus, E is the Young's modulus and σ is the Poisson's ratio:

$$A = \frac{2C_{44}}{C_{11} - C_{12}}, \quad (5)$$

$$C_s = (C_{11} - C_{12})/2, \quad (6)$$

$$B = \frac{C_{11} + 2C_{12}}{3}, \quad (7)$$

$$E = \frac{9BG}{3B + G}, \quad (8)$$

$$\sigma = \frac{3B - 2G}{2(3B + G)}, \quad (9)$$

Table 4. The calculated elastic constants of $Zn_{1-x}TM_xSe$ (TM = Mn, Fe and Co) as functions of concentration.

Compound	C_{11} (GPa)			C_{12} (GPa)			C_{44} (GPa)		
	This work	Exp.	Theor.	This work	Exp.	Theor.	This work	Exp.	Theor.
ZnSe	59.84	82.8[a], 85.9[e]	82.45[b], 84.0[c], 91.2[d]	22.46	46.2[a]	42.71[b], 49[c], 58.2[d]	31.84	41.2[a]	35.5[b], 558[c], 42.0[d]
$Zn_{0.75}Mn_{0.25}Se$	45.34			11.93			18.21		
$Zn_{0.5}Mn_{0.5}Se$	38.65			3.38			12.75		
$Zn_{0.25}Mn_{0.75}Se$	36.48			−2.07			7.51		
$Zn_{0.75}Co_{0.25}Se$	52.76			19.26			24.64		
$Zn_{0.5}Co_{0.5}Se$	49.76			13.91			18.94		
$Zn_{0.25}Co_{0.75}Se$	56.81			23.03			20.34		
$Zn_{0.75}Fe_{0.25}Se$	53.14			30.05			18.88		
$Zn_{0.5}Fe_{0.5}Se$	50.03			19.73			13.59		
$Zn_{0.25}Fe_{0.75}Se$	41.86			17.45			7.68		

[a]Ref. [45], [b]ref. [34], [c]ref. [36], [d]ref. [46], [e]ref. [47].

Table 5. The calculated values of elastic anisotropic factor A, Debye temperature θ, Young's modulus E (GPa), shear modulus G (GPa), B/G, Poisson's ratio and bulk modulus as a function of concentration for $Zn_{1-x}Mn_xSe$, $Zn_{1-x}Co_xSe$ and $Zn_{1-x}Fe_xSe$ alloys at $x = 0.25$, 0.5 and 0.75.

Alloys	ZnSe	$Zn_{1-x}Mn_xSe$			$Zn_{1-x}Co_xSe$			$Zn_{1-x}Fe_xSe$			Theor. ZnSe
		0.25	0.5	0.75	0.25	0.5	0.75	0.25	0.5	0.75	
		Our work									
A	1.703	1.08	0.72	0.390	1.47	1.05	1.20	1.75	1.08	1.02	0.91[a], 1.78[b]
$B_v/B_R/B_H$	34.92	23.671	15.142	10.775	30.431	25.868	34.295	30.303	25.741	19.079	60.7[a]
θD	262.43	221.183	202.282	178.663	239.237	224.8	226.358	254.088	229.87	220.214	88.3[a]
E_v	63.607	42.112	33.323	26.606	52.179	44.880	48.035	58.612	45.991	39.831	72.25[b]
E_R	60.253	42.053	32.696	22.813	50695	44.855	47.701	55.237	45.935	39.869	0.25[a]
E_H	61.942	42.082	33.010	24.759	51.440	44.867	47.868	56.937	45.962	39.869	0.276[b]
σV	0.196	0.195	0.133	0.088	0.214	0.210	0.266	0.177	0.202	0.151	40.5[a]
σR	0.212	0.196	0.140	0.147	0.222	0.211	0.268	0.196	0.202	0.151	29.7[a]
σH	0.204	0.196	0.136	0.117	0.218	0.210	0.267	0.186	0.202	0.151	35.1[a]
G_v	26.582	17.609	14.703	12.222	21.487	18.533	18.963	24.886	19.128	17.310	
G_R	24.848	17.578	14.339	9.944	20.737	18.520	18.807	23.089	19.099	17.309	
G_H	25.715	17.593	14.521	11.083	21.112	18.526	18.885	23.987	19.113	17.309	
B/G	1.357	1.345	1.042	0.972	1.441	1.396	1.815	1.263	1.346	1.102	

[a]Ref. [34], [b]ref. [32].

$$G_v = \frac{C_{11} - C_{12} + 3C_{44}}{5}, \tag{10}$$

$$G_R = \frac{5C_{44}(C_{11} - C_{12})}{4C_{44} + 3(C_{11} - C_{12})}, \tag{11}$$

$$G_H = \frac{G_v + G_R}{2}. \tag{12}$$

The materials studied are anisotropic in general due to the fact that the values of A are greater than 1. However, A is less than 1 for $Zn_{1-x}Mn_xSe$ compounds at 0.5 and 0.75 and so they are less rigid. The high or low B/G values are associated with ductility or brittleness [51,52]. The critical value, which separates ductile and brittle materials, is about 1.75. Therefore, according to table 5, the compounds are brittle. The Young's modulus E and the Poisson's ratio σ are also important parameters in technological applications [53,54]. They define the stiffness of a material. The Poisson's ratio σ indicates the kind of interatomic forces, where the material has ionic bonds if σ lies between 0.17 and 0.28 [55]. Our calculated values of Poisson's ratio range from 0.11 to 0.15, confirming the covalent properties of the alloys. The Young's modulus decreases when we move from 0.25 to 0.75.

4. Conclusion

We investigated the structural, electronic, magnetic, thermal and elastic properties of $Zn_{1-x}TMn_xSe$ (TM = Mn, Fe and Co) at $x = 0.25, 0.5$ and 0.75 in the zincblend ferromagnetic phases. The calculations were performed using the FP-LAPW method. The calculations predicted the nonlinear behaviour of the lattice constant, bulk modulus and band-gap dependence on x. The plots of density of states show the semiconducting behaviour of $Zn_{1-x}Mn_xSe$ and $Zn_{1-x}Co_xSe$ compounds and half-metallic behaviour with 100% spin polarisation at the Fermi level for $Zn_{1-x}Fe_xSe$ compounds. The p–d hybridisation leads to a reduction of the local magnetic moment of Mn, Co and Fe by inducing small local magnetic moment on the non-magnetic Zn and Se atoms. The compounds were found to be mechanically stable. This is suitable for spintronic applications and electronic devices. The results in this work are promising for future experimental investigations.

Acknowledgement

This work was supported by the Algerian University Research Project (CNEPRU) under No. B00L02UN 280120140051.

References

[1] I Zutic, J Fabian and S Das Sarma, *Rev. Mod. Phys.* **76**, 323 (2004)
[2] T Roy and A Chakrabarti, *Pramana – J. Phys.* **89**: 1401 (2017)
[3] S A Wolf, D D Awschalom, R A Buhrman, J M Daughton, S Von Molnar, M L Roukes, A Y Chtchelkanova and D M Treger, *Science* **294**, 1488 (2001)
[4] D Chib, M Sawicki, Y Nishitani, Y Nakatani, F Matsukura and H Ohno, *Nature* **455**, 515 (2008)
[5] T Diet, H Ohno, F Matsukura, J Cibert and D Ferrand, *Science* **287**, 1019 (2000)
[6] D A Schwartz, K R Kittilstved and D R Gamelin, *Appl. Phys. Lett.* **85**, 1395 (2004)
[7] X Liu and J K Furdyna, *J. Appl. Phys.* **95**, 7754 (2004)
[8] M Jain, *Diluted magnetic semiconductors* (World Scientific, Singapore, 1991)
[9] S M Alay-e-Abbas, K M Wong, N A Noor, A Shaukat and Y Lei, *Solid State Sci.* **14**, 1525 (2012)
[10] Ch Bourouis and A Meddour, *J. Magn. Magn. Mater.* **324**, 1040 (2012)
[11] M Sajjad, H X Zhang, N A Noor, S M Alay-e-Abbas, M Younas, M Abid and A Shaukat, *J. Supercond. Nov. Magn.* 27, 2327 (2014)
[12] M Sajjad, H X Zhang, N A Noor, S M Alay-e-Abbas, A Shaukat and Q Mahmood, *J. Magn. Magn. Mater.* **343**, 177 (2013)
[13] E Kulatov, H Nakayama, H Ohta, K Motizukid, Yu Uspenskii and H Mariette, *J. Magn. Magn. Mater.* **272**, 1911 (2004)
[14] A Deneuville, D Tanner and P H Holloway, *Phys. Rev. B* **43**, 6544 (1991)
[15] U Philipose, P Sun, T Xu, H E Ruda, L Yang and K L Kavanagh, *J. Appl. Phys.* **101**, 014326 (2007)
[16] S Zh Karazhanov, P Ravindran, A Kjekshus, H Fjellvåg and B G Svensson, *Phys. Rev. B* **75**, 155104 (2007)
[17] D J Sing, *Plane waves, pseudopotentials and the LAPW method* (Kluwer Academic Publishers, Dordrecht, The Netherlands, 1994)
[18] W Kohn and L J Sham, *Phys. Rev.* **140**, B1133 (1965)
[19] P Blaha, K Schwarz, G K H Madsen, D Kvasnicka and J Luitz, *WIEN2K, an augmented plane wave plus local orbitals program for calculating crystal properties* (Karlheinz Schwarz, Techn. Universität, Wien, Austria, 2014), ISBN633-9501031-1-2
[20] P Hohenberg and W Kohn, *Phys. Rev. B* **136**, 864 (1964)
[21] J P Perdew, S Burke and M Ernzerhof, *Phys. Rev. Lett.* **77**, 3865 (1996)
[22] F D Murnaghan, *Proc. Natl. Acad. Sci. USA* **30**, 244 (1944)
[23] E Engel and S H Vosko, *Phys. Rev. B* **47**, 13164 (1993)
[24] F Tran and P Blaha, *Phys. Rev. Lett.* **102**, 226401 (2009)
[25] O Zakharov, A Rubio, X Blase, M L Cohen and S G Louie, *J. Phys. Rev. B* **50(15)** (1994)

[26] H Kim, R Vogelgesang, A K Ramdas, F C Peiris, U Bindley and J K Furdyna, *Phys. Rev. B* **58**, 6700 (1998)
[27] W Zhou and S Wu, *J. Magn. Magn. Mater.* **395**, 166 (2015)
[28] L A Kolodziejski, R L Gunshor, N Otsuka, B P Gu, Y Hefetz and A V Nurmikko, *Appl. Phys. Lett.* **48**, 1482 (1986)
[29] L Vegard, *Z. Phys.* **5**, 17 (1921)
[30] H Yahi and A Meddour, *J. Magn. Magn. Mater.* **401**, 116 (2016)
[31] M Bilal, M Shafiq, I Ahmad and I Khan, *J. Semicond.* **35**, 072001 (2014)
[32] D Varshney, U Sharma and N Kaurav, *J. Phys.: Condens. Matter* **20**, 075204 (2008)
[33] R Khenata, A Bouhemadou, M Sahnoun, A H Reshak, H Baltache and M Rabah, *Comput. Mater. Sci.* **38**, 29 (2006)
[34] P K Saini, D Singh and D S Ahlawat, *Chalcogenide Lett*. **11**, 405 (2014)
[35] F Benkabou, H Aourag and M Certier, *Mater. Chem. Phys.* **66**, 10 (2000)
[36] B N Brahmi, A E Merad, M R Boufatah, CNPA VIII, Béjaia, 11–13 (2008)
[37] T Teshome and A Datta, *J. Phys. Chem. C* **121(28)**, 15169 (2017)
[38] K-H Hellwege and O Madelung (eds), Semi-magnetic semiconductors, In: *Landolt–Bornstein, New Series*, *Group III* (Springer, New York, 1982)
[39] H Venghaus, *Phys. Rev. B* **19**, 3071 (1979)
[40] P Dufek, P Blaha and K Schwarz, *Phys. Rev. B* **50**, 7279 (1994)
[41] F El Haj Hassan, H Akbarzadeh and S J Hashemifar, *J. Phys.: Condens. Matter.* **16**, 3329 (2004)
[42] K L Yao, G Y Gao, Z L Liu and L Zhu, *Solid State Commun.* **133**, 301 (2005)
[43] M A Blanco, E Francisco and V Luaña, *Comput. Phys. Commun.* **158**, 57 (2004)
[44] A Otero-de-la-Roza and V Luaña, *Comput. Phys. Commun.* **182**, 1708 (2011)
[45] P Ravindran, L Fast, P A Korzhavyi, B Johansson, J Wills and O Eriksson, *J. Appl. Phys.* **84**, 4891 (1998)
[46] Y A Burenkov, S Y Davydov and S P Nikanorov, *Phys. Solid State* **17**, 1446 (1975)
[47] H Y Wang, J Cao, X Y Huang and J M Huang *Condens. Matter Phys.* **15**, 13705 (2012)
[48] B H Lee, *J. Appl. Phys.* **41**, 2984 (1970)
[49] R Hill, *Proc. Phys. Soc. A* **65**, 349 (1952)
[50] W Voigt, *Lehrbush der Kristallphysik* (B.G. Taubner, Leipzig, 1928)
[51] S F Pagh, *Philos. Mag.* **45**, 823 (1954)
[52] F Peng, D Chen and X D Yang, *Solid State Commun.* **149**, 2135 (2009)
[53] A Otero-de-la-Roza, D Abbasi-Pérez and V Luaña, *Comput. Phys. Commun.* **182**, 2232 (2011)
[54] A Reuss, *Z Angew. Math. Mech.* **9**, 49 (1929)
[55] Z Charifi, H Baaziz, Y Saeed, A H Reshak and F Soltani, *Phys. Status Solidi B* **249**, 18 (2012)